Rheological Properties and Microstructures of Anionic Micellar Solutions in the Presence of Different Inorganic Salts

Jian-Hai Mu,[†] Gan-Zuo Li,*[,†] Xiao-Lei Jia,[†] Hong-Xia Wang,[‡] and Gao-Yong Zhang[‡]

Key Lab for Colloid and Interface Chemistry of State Education Ministry, Shandong University, Jinan 250100, People's Republic of China, and China Research Institute of Daily Chemical Industry, Taiyuan 030001, People's Republic of China

Received: November 8, 2001; In Final Form: August 4, 2002

Wormlike micelles, obtained firstly in anionic surfactant sodium dodecyl trioxyethylene sulfate (SDES) solutions in the presence of $AlCl_3$, were studied using zero-shear viscosities and freeze-fracture TEM micrographs. Then the effects of inorganic salts with different cations, $AlCl_3$, $MgCl_2$, $CaCl_2$, and NaCl, on the rheological properties and microstructures of the SDES micellar solutions were investigated generally. The steady-shear viscosity followed the Cross empirical equation, and the dynamic vlscoelasticity was well modeled by the simple Maxwell model. There exists an optimal molar ratio R_m of surfactant to salt at which the micelles reach maximum growth. We find $R_m \leq 1/5$ for SDES/NaCl system, and $R_m \approx 1/3$ for the other three systems. Variations in the surfactant packing parameter R_p help explain the changes of rheology and microstructure of the solutions, according to the cationic radii and charges and the interaction between the cations and surfactant molecular headgroups. The ability of cations that make the micelles reach a maximum growth followed the order of $Al^{3+} > Mg^{2+} > Ca^{2+} > Na^+$.

1. Introduction

Rheological studies are vital in many industrial applications, including food emulsions, cosmetics, paints, agrochemicals, pharmaceuticals, bitumen emulsions, inks and paper coatings, adhesives, and many household products.[1] The rheological properties are functions of both the structural arrangement of particles and the various interaction forces which operate in the system.[2] It is now well-known that the addition of salt to aqueous cationic surfactant solutions weakens electrostatic interactions and causes micellar growth, in which the micelles undergo a transition from spherical, rodlike, to larger cylindrical aggregates or flexible wormlike micelles. The reported systems mainly include cetylpyridinium halide (CPyX),[3−8] cetyltrimethylammonium halide (CTAX)[8−15] or some other cationic surfactants,[16−18] with aromatic counterions or halide anions. Some nonionic surfactants can also form wormlike micelles under certain conditions.[19−21] Wormlike micelles consist of highly flexible locally cylindrical aggregates (typical diameter is 2−5 nm and persistent length is 15−20 nm) with an average length approaching 1 μm.[22] Such micellar solutions have high surface activity and high viscoelasticity, which make them useful in many fields. However, the formation of anionic wormlike micelles and their rheological properties and microstructures have been less intensively investigated,[23] which badly restricts the development of the theory of wormlike micelles and their application in enhanced oil recovery (EOR) and some industrial fields. Most of all, it is not clear which structures and ratios for ionic surfactants and counterions can form wormlike micelles. Therefore, many investigations should be done to enrich the theory and application of wormlike micelles.

In this work, rheological methods and freeze-fracture transmission electron microscopy (FF-TEM) were applied to investigate the micellar growth, steady and dynamic rheological properties, and microstructures of the aqueous anionic surfactant solutions, sodium dodecyl trioxyethylene sulfate (SDES), in the presence of different inorganic salts, $AlCl_3$, $CaCl_2$, $MgCl_2$, NaCl, etc. The effect of different counterions on the microstructures of the aggregates was discussed according to the point of surfactant packing parameter. Some interesting and noticeable conclusions were obtained.

2. Experimental Section

Materials and Sample Preparation. The anionic surfactant sodium dodecyl trioxyethylene sulfate (SDES), $CH_3(CH_2)_{11}(OCH_2CH_2)_3OSO_3Na$, was purchased from Henkel Ltd. (Germany). It was recrystallized three times from ethanol and characterized by the melting point (148−150 °C) and cmc (2.5×10^{-3} M, close to the reported values in ref 24, 2.8×10^{-3} M, and ref 25, 2.3×10^{-3} M). All inorganic salts, $AlCl_3$, $CaCl_2$, $MgCl_2$, and NaCl, were analytical reagent grade (Shanghai Chemical Co., China). All the micellar solutions were prepared by using double distilled water, and were left to stand for 2 days to reach equilibrium. There were no air bubbles in the solutions.

Rheological Measurements. The rheological experiments were carried out on a controlled stress rheometer (HAAKE RS 75) with a cone-plate sensor (35 mm diameter, 2° angle). The sample thickness in the middle of the sensor was 0.105 mm. A solvent trap was used to avoid evaporation. Experiments were performed at temperatures between 25 and 40 °C with a maximum deviation of ±0.1 °C. Except as noted, experiments were performed at 25.0 ± 0.1 °C. The viscosity η of the samples was obtained from steady-shear measurements with the shear rate ranging from 0.3 to 500 s^{-1}. Frequency sweep measurements were performed at a given stress σ_0 (chosen in the linear

* To whom correspondence should be addressed. Email: coliw@sdu.edu.cn. Tel: +86-531-8564750.

[†] Key Lab for Colloid and Interface Chemistry of State Education Ministry.

[‡] China Research Institute of Daily Chemical Industry.

10.1021/jp014096a CCC: $22.00
Published on Web 10/10/2002

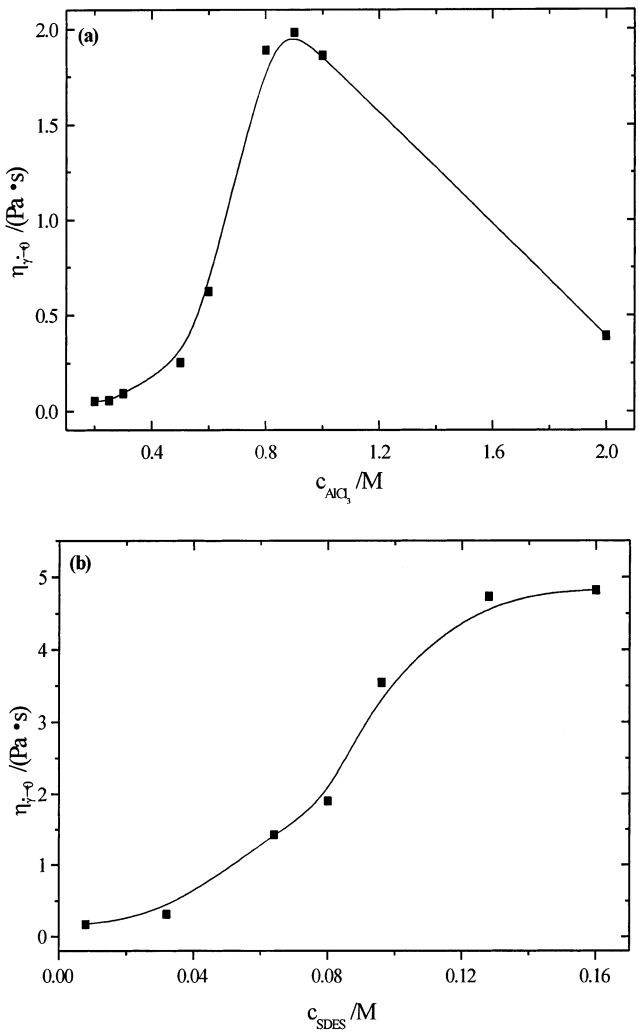

Figure 1. Zero-shear viscosity as a function of $AlCl_3$ (a) and SDES (b) concentrations at 30 °C.

domain where the amplitude of the deformations is very low) in the frequency (ω) region varying from 0.06 to 100 rad·s^{-1}.

Freeze-Fracture TEM. The FF-TEM investigation was carried out using a freeze fracture apparatus (Eiko Model FD-2A) on a nitrogen-cooled support and a TEM (JEOL Model JEM-1200EX). The procedure has been described in several literatures.[26−28] A thin layer of the sample (20−30 μm) was placed on a thin copper holder and then rapidly quenched in liquid nitrogen. The frozen sample was fractured at −140 °C, in a high vacuum better than 10^{-5} Pa with the liquid nitrogen cooled knife in the freeze etching unit. Increasing the temperature to −95 °C and keeping the high vacuum, the fractured sample was placed 30−60 min in order to evaporate the water adsorbed in the surface of the sample. Then decreasing the temperature to −120 °C again, the replication was done using unidirection shadowing at an angle of 45°, with platinum-carbon (Pt−C) and 1−10 nm of mean metal deposit. The replicas were washed with double distilled water and were observed in transmission electron microscope.

3. Results

Formation of Wormlike Micelles. The zero-shear viscosity $\eta_{\dot{\gamma}\to 0}$ of the SDES/$AlCl_3$ solutions was measured as functions of surfactant and salt concentrations at 30 °C. The results of these measurements are shown in Figure 1. In Figure 1a, on increasing $AlCl_3$ concentration, with a fixed SDES concentration of 0.08 M, the viscosity shows first a slow increase and then a sharp increase at 0.4−0.5 M $AlCl_3$ until a maximum of 1.9 Pa·s at a salt concentration of 0.8−0.9 M, and finally a dramatic decreases. This behavior is expected. It is similar to the behavior obtained in several aqueous surfactant/salt systems[14] and is explained by the formation and breaking of wormlike micelles. It is generally known that at fixed surfactant concentration, an increase in the salt content leads to a micellar growth, because of enhanced screening of the electrostatic interactions. At a low salt content, rodlike micelles may form and grow, which will increase the viscosity of the solution by a small amount. When the length of the rodlike micelles has increased further so that they are flexible and can curve freely, the micelles become wormlike, which can result in a rapid increase in viscosity. Finally, at very high salt concentration, the wormlike micelles may break into several pieces,[14] and at the same time, salting-out occurs so that the content of surfactant in the bulk solution decreases, and so the viscosities of the solutions become lower.

The effect of the surfactant concentration on zero-shear viscosity of 0.8 M $AlCl_3$ solutions is illustrated in Figure 1b. The curve can be divided into three domains: at low SDES concentration (below 0.04 M), $\eta_{\dot{\gamma}\to 0}$ shows little change, and then increases until a maximum of 4.8 Pa·s at an SDES content of 0.12 M, and finally it increases slowly or remains constant for higher SDES concentrations. This can also be explained from the viewpoint of micellar growth. At lower concentrations, increasing SDES only leads to an increase of the size and number of rodlike micelles, and then an increase in micellar length and the formation of wormlike micelles, finally entangled network structures occur at a certain surfactant concentration. However, at a higher SDES content, viscosity shows less dependent on surfactant concentration, owing to the equilibrium between combination and dissociation of the aggregates.

To make sure of the formation of wormlike micelles and network structures in SDES/$AlCl_3$ solutions, the freeze-fracture TEM is applied to investigate the structure. The application of the freeze-fracture TEM to the study of the microstructure of complex fluids, like microemulsions, wormlike micelles and dilute lamellar systems, has been recently demonstrated.[11,26−31] Figure 2 shows FF-TEM micrographs of the vitrified samples with different SDES concentrations (0.032, 0.08, and 0.128 M) and a fixed $AlCl_3$ content of 0.8 M. Figure 2a shows some spherical and rodlike structures, and there are not any wormlike micelles in the system of 0.032 M SDES/0.8 M $AlCl_3$, which is consistent with the result obtained from Figure 1, and therefore the viscosity is very small.

Figure 2b and c shows electron micrographs of the sample 0.08 M SDES/0.8 M $AlCl_3$ where wormlike micelles have begun forming according to our interpretation of the data in Figure 1. Figure 2b is an image with a magnification 2×10^4 of the sample showing many flexible wormlike structures, which we interpret as wormlike micelles. Some micelles entangle with each other and form weak network structures. It can also be observed that there are several "clusters faces", including many wormlike micelles with different arrangement orientation. In each "cluster face", the wormlike micelles are in the same direction. The crossed polarizer and optical microscope investigations show that the samples are isotropic, not lyotropic liquid crystals. The well-arranged structure of wormlike micelles would be broken into a mixed and disorderly state by shearing, so that more and more micelles can present a further entanglement and the relatively obvious network structure will be formed. Figure

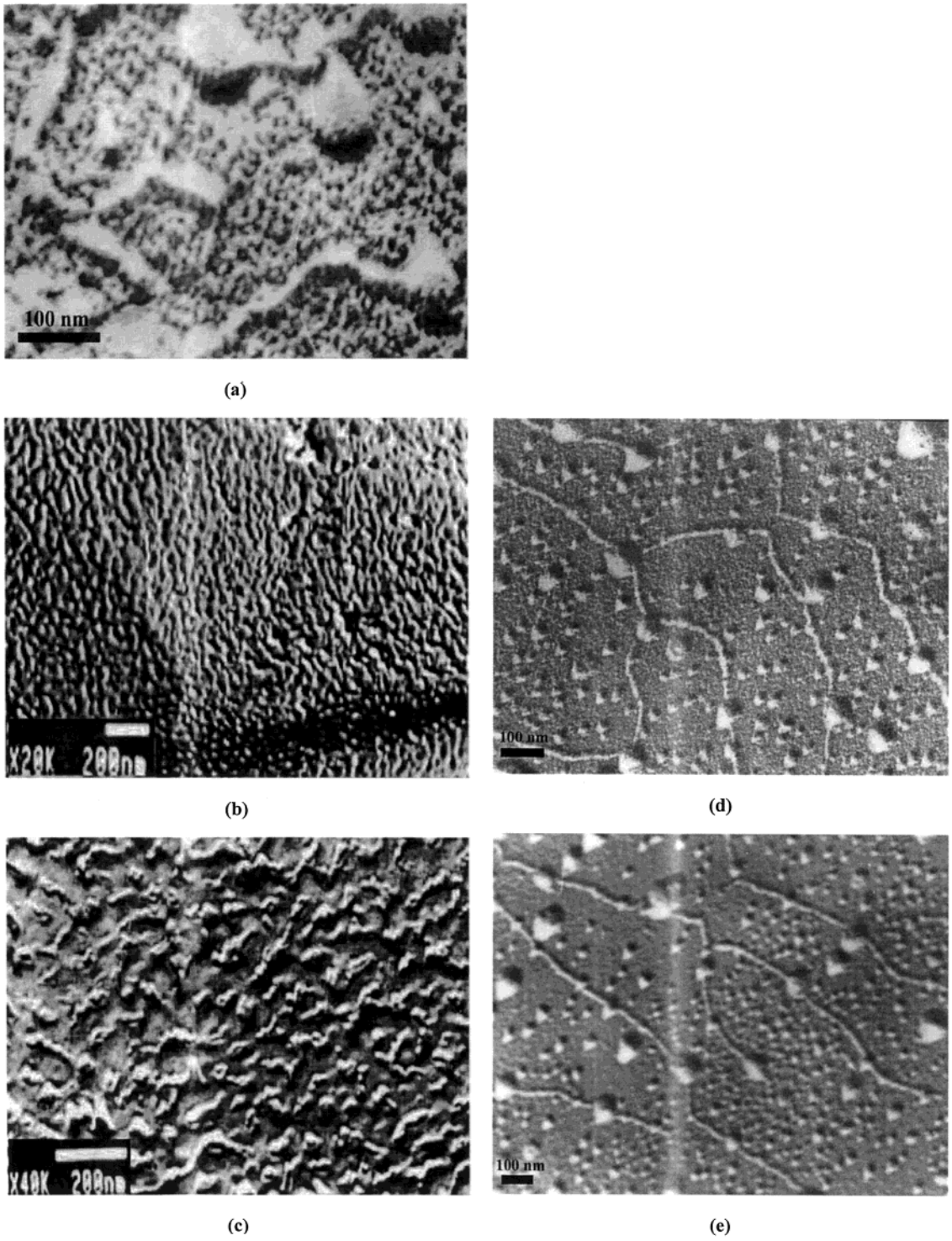

Figure 2. (a−e) FF-TEM micrographs of 0.032 M (a), 0.08 M (b, c), and 0.128 M (d, e) SDES solutions in the presence of 0.8 M $AlCl_3$.

2c is an image with a magnification 4×10^4, in which the flexible wormlike micelles and local network structures can be observed distinctly. The micelles are approximately 5−10 nm in diameter and 100−200 nm in length in general, and the longest "worm" is about 400 nm. The ratio of length and diameter is almost larger than 10. In addition, the existence of some spherical and rodlike particles in the image shows that the wormlike micelles have not been formed completely in the sample, resulting in the lower zero-shear viscosity (about 2.0 Pa·s) of the solution. The acceptable reason is that the concentration of surfactant in the sample is so low that the interesting structure cannot be formed perfectly.

Parts d and e of Figure 2 show electron micrographs of the sample 0.128 M SDES/0.8 M $AlCl_3$ where the equilibrium between combination and dissociation of aggregates occurs according to Figure 1. It is can be seen that there are some long threadlike (wormlike) structures, approximately 10 nm in diameter, with lengths that are hard to determine from the images but at least in one instance the lengths exceed 1 μm. At the same time, there are some larger spherical aggregates near the wormlike micelles, and they are about 50−100 nm in diameter. This may be the partially dissociated wormlike aggregates, since there cannot exist so large spherical micelles. Furthermore, there are many small spheroids (less than 10 nm

in diameter) in the images, which should be considered as sphere-like micelles.

According to the FF-TEM micrographs of the samples, we can obtain the reason that the viscosity of the studied solutions is far smaller than that of some cationic wormlike micelles. For the latter, the images show more flexible wormlike micelles (even several microns in length) and entangled network structures, so its viscosity can reach 100−1000 Pa·s.[11,12]

It can be concluded from the results of Figures 1 and 2 that there is an optimal concentration for the surfactant and inorganic salt, in other words, there exists an optimal molar concentration ratio of the surfactant to the salt R_m, in which the wormlike micelles will be formed completely and the viscosity of the solution will be largest. Therefore, R_m will be investigated thoroughly as follows, for SDES solutions in the presence of different inorganic salts by steady-shear viscosity and dynamic viscoelasticity measurements.

Effect of Inorganic Salts on Steady Shear Viscosity. Figure 3 shows the steady-shear viscosity as a function of shear rate for SDES/$AlCl_3$ solutions. In Figure 3a, the concentration of SDES increases from 0.1 to 0.25 M with $R_m = {}^1/_2$ at 25 °C. The viscosity is approximately constant with an increasing shear rate at low rates; however, after a critical rate, the viscosity decreases dramatically. The plateau viscosity increases with SDES concentration. Figure 3b is the shear viscosity curves for 0.2 M SDES solutions with different R_m, ${}^1/_5$−${}^1/_1$, at 25 °C. Similar to Figure 3a, there exists the viscosity plateau at low shear rate, which is relative to R_m. Figure 3c shows the shear viscosity for 0.2 M SDES solution with $R_m = {}^1/_2$ at different temperature. The viscosity plateau occurs, too, and decreases with the increase of the temperature.

The results in Figure 3 follow the Cross empirical equation, which fits curves with two plateaus separated by a power-law region:[32]

$$\eta = \eta_{\dot\gamma\to\infty} + \frac{\eta_{\dot\gamma\to 0} - \eta_{\dot\gamma\to\infty}}{1 + (\dot\gamma/\dot\gamma_b)^n} \qquad (1)$$

$\eta_{\dot\gamma\to 0}$ and $\eta_{\dot\gamma\to\infty}$ are the viscosities at zero-shear rate and infinite shear rate, respectively. $\dot\gamma_b$ is the constant rate parameter, and n is the rate power-law index. The drawn lines in Figure 3 are calculated from the fitted parameters. It can be found that all experiment points are consistent on the whole, except for the viscosity at higher shear rate because there is not evident plateau, which results in an inaccurate $\eta_{\dot\gamma\to\infty}$ value obtained from Cross equation, and the infinite shear viscosity will not be discussed in this study.

The results of the steady-shear curve fit for SDES solutions in the presence of different inorganic salts, $AlCl_3$, $CaCl_2$, $MgCl_2$, and NaCl, are given in Table 1. The following rules can be obtained from Table 1:

(i) Fixed R_m, increasing SDES concentration, $\eta_{\dot\gamma\to 0}$ and n increase, and $\dot\gamma_b$ decreases.

(ii) Increasing temperature, $\eta_{\dot\gamma\to 0}$ and n decrease, and $\dot\gamma_b$ increases.

(iii) Fixed SDES concentration, increasing R_m, $\eta_{\dot\gamma\to 0}$ and n will reach a maximum and $\dot\gamma_b$ a minimum at $R_m \approx {}^1/_5$ for NaCl system and $R_m \approx {}^1/_3$ for other systems.

There is a uniform rule that for one SDES/salt system, the higher $\eta_{\dot\gamma\to 0}$, the smaller $\dot\gamma_b$, the larger n. The rate parameter $\dot\gamma_b$ can be assumed as the critical shear rate at which the viscosity varies from a plateau to a rapid decrease, which indicates the intensity that the microstructures of the sample can support by the action of shearing. The rate index n shows the sharpness that the viscosity changes as increasing shear rate, which indicates the speed that the microstructures of the sample can be changed by the action of shearing. According to Figures 1

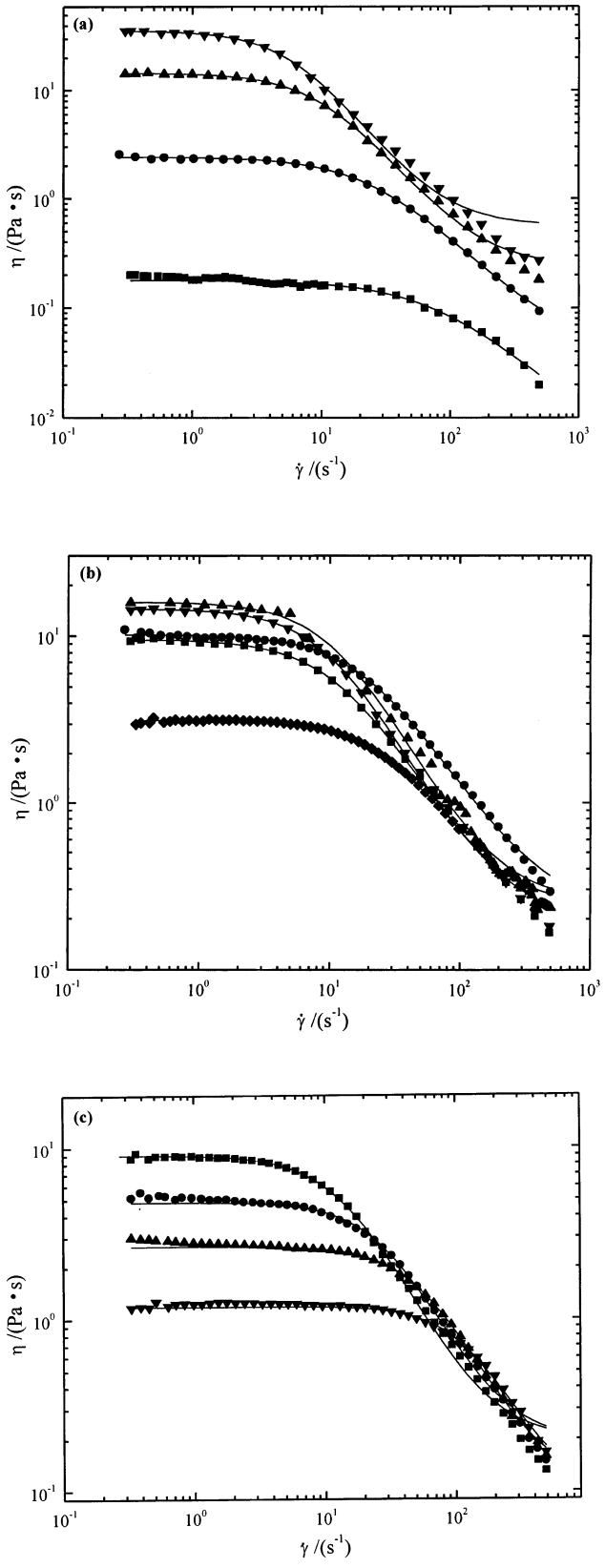

Figure 3. (a−c) Steady shear viscosity as a function of shear rate for SDES/$AlCl_3$ solutions. (a) $R_m = {}^1/_2$, c_{SDES}/M = 0.1 (■), 0.15 (●), 0.2 (▲), 0.25 (▼); (b) c_{SDES} = 0.2 M, $R_m = {}^1/_5$ (■), ${}^1/_4$ (●), ${}^1/_3$ (▲), ${}^1/_2$ (▼), ${}^1/_1$ (◆); (c) c_{SDES} = 0.2 M, $R_m = {}^1/_2$, temperature/°C = 25.0 (■), 30.0 (●), 35.0 (▲), 40.0 (▼).

TABLE 1: Steady Shear Viscosity Parameters for SDES Solutions Obtained from Cross Equation

c_{SDES}/c_{salt} (M/M)	$\eta_{\dot{\gamma}\to 0}$ (Pa·s)	$\eta_{\dot{\gamma}\to\infty}$ (Pa·s)	$\dot{\gamma}_b$ (s^{-1})	n	c_{SDES}/c_{salt} (M/M)	$\eta_{\dot{\gamma}\to 0}$ (Pa·s)	$\eta_{\dot{\gamma}\to\infty}$ (Pa·s)	$\dot{\gamma}_b$ (s^{-1})	n
SDES/$AlCl_3$					SDES/$MgCl_2$				
0.1/0.2	0.18	0.0035	85.2	1.13	0.1/0.2	0.018			
0.15/0.3	2.41	0.043	27.34	1.28	0.15/0.3	0.21	0.017	113.8	1.01
0.2/0.4	14.39	0.25	10.41	1.53	0.2/0.4	10.58	0.12	6.89	1.48
30 °C	9.79	0.18	17.00	1.48	30 °C	6.02	0.22	13.97	1.46
35 °C	4.02	0.084	39.42	1.44	35 °C	4.42	0.063	31.47	1.38
40 °C	1.87	0.051	79.35	1.09	40 °C	2.85	0.14	48.64	1.18
0.25/0.5	35.74	0.61	5.97	1.60	0.25/0.5	30.63	0.37	6.03	1.51
0.2/1.0	9.51				0.2/1.0	23.05	0.32	7.96	1.40
0.2/0.8	10.20	0.22	21.39	1.35	0.2/0.8	25.43	0.30	6.11	1.50
0.2/0.6	15.70	0.23	9.50	1.55	0.2/0.6	27.68	0.38	5.6	1.56
0.2/0.2	3.15	0.35	30.54	1.25	0.2/0.2	0.31			
0.2/0.1	0.90				0.2/0.1	0.035			
0.2/0.05	0.13				0.2/0.05	0.017			
SDES/$CaCl_2$					SDES/NaCl				
0.1/0.2	0.084	0.028	137.3	1.09	0.15/0.6	0.14			
0.15/0.3	1.43	0.074	37.62	1.46	0.2/0.8	8.89	0.28	10.71	1.52
0.2/0.4	8.95	0.23	14.49	1.65	30 °C	4.08	0.10	24.52	1.43
30 °C	5.19	0.047	26.97	1.55	35 °C	2.44	0.095	46.00	1.37
35 °C	2.77	0.037	57.63	1.52	40 °C	1.17	0.13	79.25	1.21
40 °C	1.23	0.0036	135.2	1.46	0.25/1.0	14.68	0.31	8.58	1.56
0.25/0.5	23.81	0.50	8.81	1.69	0.2/1.0	14.33	0.25	10.38	1.53
0.2/1.0	5.17	0.19	34.04	1.53	0.2/0.6	1.06			
0.2/0.8	11.68	0.24	15.34	1.63	0.2/0.4	0.011			
0.2/0.6	12.77	0.20	12.63	1.66					
0.2/0.2	1.42								
0.2/0.1	0.028								
0.2/0.05	0.008								

and 2, the wormlike micelles with more flexible structure and larger ratio of length to diameter, will appear in the solution with higher viscosity. The longer size of wormlike micelles makes them break into pieces or other aggregates more easily, resulting in a decrease in viscosity at low shear rate. However, for the solutions with lower viscosity, there exist many rodlike or spherical micelles which have a better elastic and can endure a higher shear. Typically, most dilute solutions of spherical micelles flow as the Newtonian fluids, whose viscosities are independent of shear rates.

Effect of Inorganic Salts on Dynamic Viscoelasticity. Before carrying out any oscillatory measurements each sample was checked to ensure measurements were made within the linear viscoelastic region where the complex G^*, storage G', and loss G'' moduli are independent of the applied stress.[33−35] For subsequent dynamic experiments we chose a stress value in the linear region.

In Figure 4a, the dynamic shear storage and loss moduli of 0.2 M SDES/$AlCl_3$ system with different R_m are shown as a function of frequency. All curves describing G' and G'' cross as the frequency increases, indicating that the materials are more elastic than viscous at high frequencies. Storage modulus above the intersection tends to level off and approach plateau values G_0, suggesting the existence of an entangled network in the solution.[16] It is sometimes difficult to determine how "good" a Maxwell model fits the data from plots of and G' versus ω. A Cole−Cole plot (plot of G'' as a function of G') provides a better picture of how well the data correspond to a single relaxation time Maxwell model, which exhibits the semicircle characteristic of a Maxwell fluid. It can be expressed as eq 2 according to Maxwell model:[1]

$$G''^2 + \left(G' - \frac{G_0}{2}\right)^2 = \left(\frac{G_0}{2}\right)^2 \qquad (2)$$

Figure 4b shows Cole−Cole plots from the data presented in Figure 4a. It is evident that most of experiment points are consistent with the fitting curves, indicating the solutions are linear viscoelastic fluids in accord with a Maxwell model having a single relaxation time. The Cole−Cole plots obtained from frequency measurements for 0.2 M SDES solutions in the presence of different inorganic salts are summaried in Figure 5. These plots all almost have semicircular shapes and the systems can be considered as Maxwell fluids, except that, at high frequencies, the shapes of some curves are altered and show some deviations from semicircles. This phenomenon has been found in many viscoelastic surfactant solutions,[11−14,36] which indicates that the microstructures in the solutions and their viscoelasticity have some changes because of the high-frequency oscillation.

Dynamic properties of the surfactant solutions are greatly influenced by the excess free counterion in the surfactant solution.[18] Candau et al.[37] reported a set of nicely fit Cole−Cole plots for semidilute (∼0.16 M) wormlike micellar solutions of dodecyltrimethylammonium bromide/NaCl with NaCl concentrations from 0 to 0.16 M. However, Clausen et al.[11] reported deviation from Maxwell behavior for solutions of CTAC (0.05 M)/NaCl (010 M) with differing concentrations of NaSal. To make a further analysis for the dynamic viscoelasticity and the Cole−Cole plots of SDES systems, two parameters were put forward. (i) The frequency ω_i in which G' and G'' appear to intersect. The higher the intersection frequency ω_i, the more difficult the formation of wormlike micelles and network structures.[38] (ii) The plateau modulus G_0 is the storage modulus value at high frequency, indicating the intrinsic elastic properties of the sample. Furthermore, a relaxation time τ can be calculated from the plateau modulus G_0 and the zero-shear viscosity $\eta_{\dot{\gamma}\to 0}$:

$$\tau = \frac{\eta_{\dot{\gamma}\to 0}}{G_0} \qquad (3)$$

which shows the speed of the structural relaxation in the sample. Table 2 lists the above three parameters for SDES/salts solutions.

It can be seen from Table 2 and Table 1 that samples with higher viscosity have a small ω_i for one system, in which the

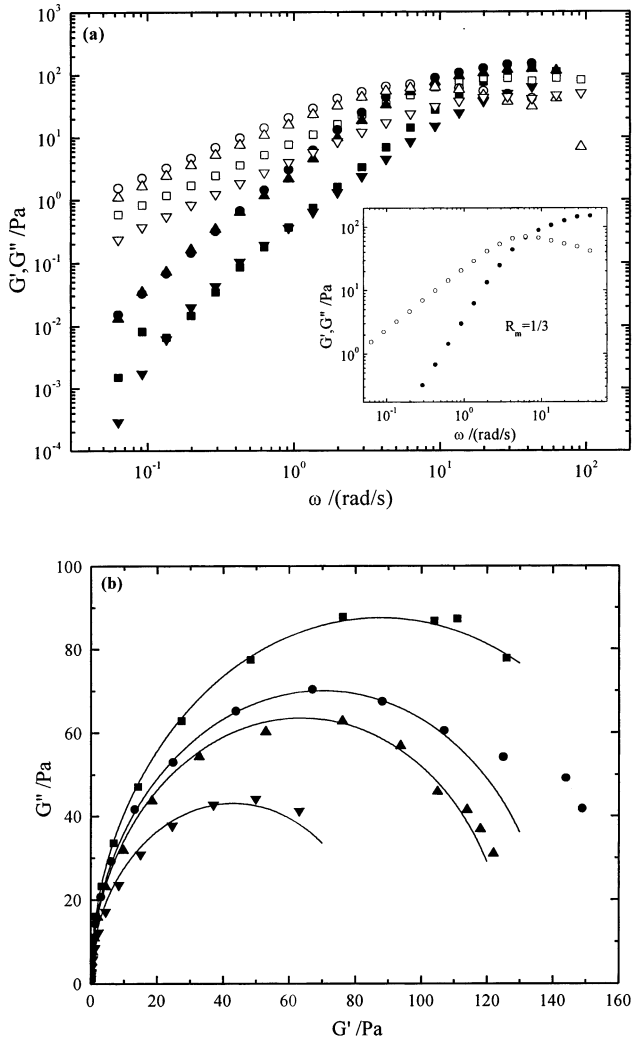

Figure 4. (a,b) (a) Storage (solid) and loss (hollow) moduli as a function of angular frequency and (b) Cole−Cole plot for 0.2 M SDES/$AlCl_3$ system with different R_m = $^1/_4$ (■ □), $^1/_3$ (● ○), $^1/_2$ (▲ △), $^1/_1$ (▼ ▽).

formation of wormlike micelles and network structures is easy and complete. The higher the viscosity, the longer the relaxation time, which can be explained by a model developed by Cates.[38] In this model, the wormlike micelles are taken as linear and flexible. The structural relaxation is determined not only by the diffusion, but also by the dissociation/recombination of aggregates. In the samples with higher viscosity, the processes of diffusion and dissociation/recombination both are slower, resulting in a slower structural relaxation and a longer relaxation time. For 0.2 M SDES solutions, the plateau modulus increases as salt content, which shows the elastic property of the sample becomes more and more evident with the increase of salt concentration. This is different from the viscous property which has a maximum. It is difficult to give an accurate explanation for the phenomenon that G_0 still increases as salt concentration after the point that maximizes the viscosity and makes the wormlike micelles form completely. Although the dissociation of wormlike micelles occurs, the new aggregates may have a higher elasticity than the former, which leads to a larger radius in the Cole−Cole curves (Figures 4 and 5) at a higher salt concentration.

The effects of different inorganic salts on these parameters are more complicated. For 0.2 M SDES/salt system, (i) for R_m = $^1/_4$, $MgCl_2$ system has the smallest ω_i and the largest τ, and

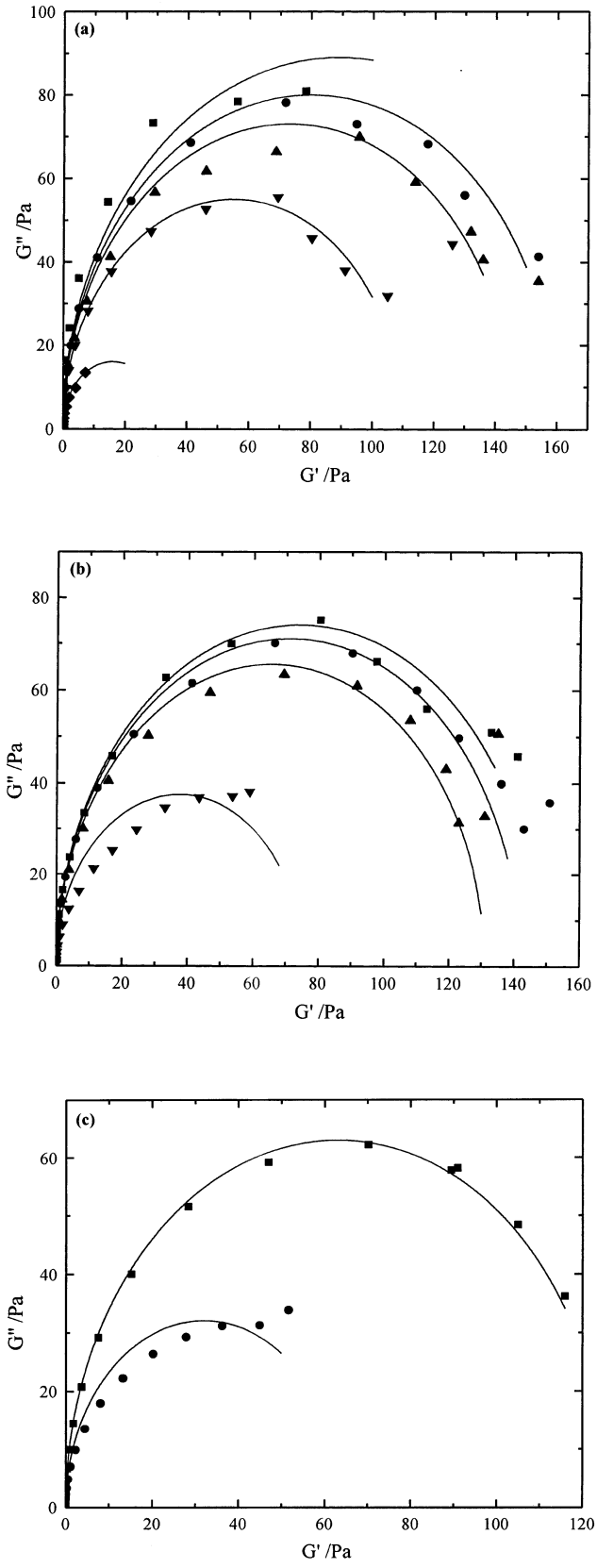

Figure 5. (a−c) Cole−Cole plots for 0.2 M SDES/$CaCl_2$ (a), $MgCl_2$ (b), and NaCl (c) solutions with different R_m = $^1/_5$ (■), $^1/_4$ (●), $^1/_3$ (▲), $^1/_2$ (▼) $^1/_1$ (◆).

$AlCl_3$ system has the largest ω_i and the smallest τ; (ii) for R_m =$^1/_3$, $MgCl_2$ the smallest ω_i and the largest τ, and $CaCl_2$ the largest ω_i[4] and the smallest τ; (iii) for R_m = $^1/_2$, $AlCl_3$ the smallest ω_i and $CaCl_2$ the largest ω_i. At the same time, for 0.2

TABLE 2: The Intersection Frequency ω_i, Plateau Modulus G_0, and Relaxation Time τ

c_{SDES}/c_{salt} (M/M)	(ω_i (rad/s)	G_0 (Pa)	$10^3\,\tau$ (s)	c_{SDES}/c_{salt} (M/M)	ω_i (rad/s)	G_0 (Pa)	$10^3\,\tau$ (s)
SDES/$AlCl_3$				SDES/$CaCl_2$			
0.15/0.3	15.2	52	46.3	0.2/1.0	42.6	178	29.0
0.2/0.4	7.6	127	113.3	0.2/0.8	13.8	160	73.0
30 °C	13.5	132	74.2	0.2/0.6	9.0	146	87.5
35 °C	29.8	128	31.4	0.2/0.4	9.7	110	81.4
40 °C	67.1	124	15.1	0.2/0.2	32.8	32	44.4
0.25/0.5	6.3	170	210.2				
0.2/0.8	24.1	175	58.3				
0.2/0.6	6.4	140	112.1				
0.2/0.2	24.2	86	36.6				
SDES/NaCl				SDES/$MgCl_2$			
0.2/1.0	7.6	126	113.7	0.2/1.0	8.2	148	155.7
0.2/0.8	15.6	64	138.9	0.2/0.8	4.5	142	179.1
				0.2/0.6	5.6	131	208.2
				0.2/0.4	13.8	75	141.1

M SDES/NaCl system, if $R_m > 1/4$, G' and G'' cannot cross within the studied frequency range, indicating a very large ω_i value. On the whole, it is easier to form wormlike micelles and network structures for SDES solution in the presence of $AlCl_3$ or $MgCl_2$, and difficult for SDES/NaCl system.

4. Discussion

The addition of inorganic salts to ionic surfactant solutions can change their microstructures and enhance micellar growth under some proper circumstances. For the anionic surfactant SDES, the effect of inorganic salts with different metal cations on the rheological properties and microstructures of the systems is different. The surfactant packing parameter R_p[39] will be used to give a qualitative explanation for the phenomenon. The packing parameter is defined via

$$R_p = \frac{V_o}{A_h L_o} \tag{4}$$

where A_h is the area at the micellar surface of surfactant headgroup(s), and L_o and V_o are the length and volume of completely extended hydrophobic tail(s). R_p is the fundamental geometric quantity for several of the possible aggregation shapes.[39] For example, critical conditions for the formation of spherical, cylindrical, bilayer, or inverted structures are $R_p \leq 1/3$, $1/3 \leq R_p \leq 1/2$, $1/2 \leq R_p \leq 1/1$, $R_p \geq 1$, respectively. Surfactants with smaller headgroup areas (high R_p) tend to form larger aggregates. A_h for cationic quaternary surfactants, such as CTAX and CPyX, is smaller than that of sulfate anionic surfactants such as SDS and SDES, which make it easier for the former to form wormlike micelles than the latter.

The spherical micelles are dominant in SDES dilute solutions without inorganic salts. In the presence of inorganic salt, there exist strong electrostatic interactions between the cation of the salt and the surfactant molecules and micellar particles, which compresses the hydration layer of surfactant headgroups and the electric double layer of micelles, resulting in a decrease in A_h and an increase in R_p. Consequently, the addition of salt enhances micellar growth. The size of metal cation is far smaller than that of surfactant headgroup, and several cations can be adsorbed in one surfactant headgroup, which makes the amount of cations must be larger than the amount of SDES, i.e., $R_m < 1$, so that the micelles will reach a maximum growth. For SDES/NaCl system, $R_m \leq 1/5$, and for other three systems, $R_m \approx 1/3$, the viscosity will reach a maximum (Table 1). Figure 6 gives a schematic diagram of the wormlike micelles. But for cationic quaternary surfactant solutions, the amount of the added inorganic anion is closer to that of surfactant in general, owing to the closer size for the inorganic anion and the surfactant headgroup.

The variation in the effect of different inorganic salts on the structure of anionic surfactant solutions mainly attributes to the difference of the interaction between the different cations of salts and the surfactant headgroups. For the cations with the same charges, the adsorption quantity of the cation with smaller radius in the micelles is higher than that with larger radius, because the cations not only can be adsorbed in the interface of the micelles, but also may be embed around the headgroups, as shown in Figure 6. Therefore, the small cation will compress the area of surfactant headgroups to a great extent and enhance micellar growth. The radii of the four studied cations are Na^+ 95, Mg^{2+} 65, Ca^{2+} 99, and Al^{3+} 50 pm, respectively.[40] The radius of Mg^{2+} is smaller than that of Ca^{2+}, resulting in a more growth extent and a higher viscosity of micelles for SDES solutions in the presence of the former. In addition, the effect of KCl on SDES micelles has also been studied, and it was found that the viscosity of the solution increased a little in the presence of KCl, i.e., 0.29 Pa·s for 0.2 M SDES with $R_m = 1/4$. It is far smaller than the viscosity of 0.2 M SDES/0.8 M NaCl solution, just because the radius of K^+ (133 pm)[40] is larger than Na^+.

The SDES molecular headgroup is a monovalent anion, and an equal amount of any of the singly charged cations will make the net charge of the micellar interface zero. This is changed when multiply charged cations are used. The radii of Al^{3+} and Mg^{2+} are smaller than that of Na^+. However, the charges of the former are greater than the latter, which makes the number of multiply charged cations adsorbed to the micellar surface and around the surfactant headgroups smaller than that of the singly charged cations. Consequently, the optimal R_m ($\approx 1/3$) for SDES solutions in the presence of Al^{3+} and Mg^{2+} is larger than that of Na^+ ($\leq 1/5$).

For Al^{3+} and Mg^{2+}, the former has a smaller radius and more charges, so that it will be relatively easier to enhance micellar growth at lower salt concentration, i.e., $R_m \geq 1/2$. At high salt content, i.e., $R_m \leq 1/3$, the ability of enhancing micellar growth becomes relatively stronger for Mg^{2+} than that of Al^{3+} because of the sharp electrostatic repulsion and the higher hydrolysis degree.

Certainly, the structure of the surfactant molecules plays a very important role for the formation of wormlike micelles. We have investigated some other anionic surfactants, such as sodium dodecyl sulfate (SDS), sodium alkyl sulfonate (AS), sodium dodecyl benzene sulfonate (SDBS), etc., and the addition of the same inorganic salts as this study cannot make the viscosity

R_m: 1/5 (■), 1/4 (●), 1/3 (▲), 1/2 (▼), 1/1 (◆).

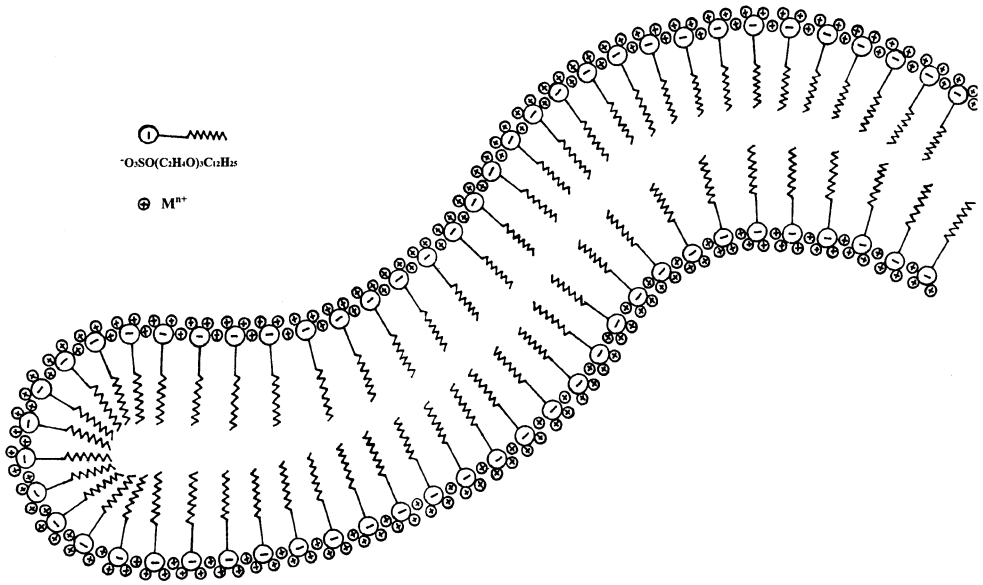

Figure 6. Schematic diagram of wormlike micelle induced by SDES solution in the presence of inorganic salt.

of the system show an evident increases, indicating that it may be difficult to form the wormlike micelles in these anionic surfactant/salt solutions. However, the condition is different for the studied systems because of the existence of oxyethylene chain ($-OCH_2CH_2-$) near the anionic polar head ($-OSO_3^-$), which is hydrophilic and can be considered as one part of the headgroup of the molecule. In the presence of inorganic salts, the counterions will not only mostly exist in the micellar surface, but also in the inside of the headgroup close to the oxyethylene chain, which can enhance the efficiency and ability for the counterions to make the micelles grow remarkably.

5. Conclusions

Rheological properties and microstructures of the SDES solutions in the presence of inorganic salts with different counterions, Al^{3+}, Mg^{2+}, Ca^{2+}, and Na^+, are studied. The following conclusions can be obtained.

(i) It is found by zero-shear viscosity measurements and freeze-fracture TEM microscopy that wormlike micelles form in SDES/$AlCl_3$ solutions of the proper surfactant and salt concentrations. However, there are still many spherical and rodlike micelles and some other aggregates in the solutions.

(ii) The steady-shear viscosity of the SDES/salt solution shows a Newtonian plateau at low rates, and can be described by the Cross empirical equation.

(iii) The Maxwell model and Cole−Cole plot were applied to determine the dynamic viscoelasticity. The wormlike micellar solutions are linear viscoelastic fluids in accord with Maxwell model having a single relaxation time. Three parameters, i.e., intersection frequency ω_i, plateau modulus G_0, and relaxation time τ, were also be discussed to analyze the processes of micellar growth, diffusion, and dissociation/recombination.

(iv) The difference of the effect of different inorganic salts on the structure of anionic surfactant solutions mainly attributed to the difference of the interaction between the different cations of salts and the surfactant headgroups, which can be explained according to the viewpoint of packing parameter R_p. There is an optimal molar ratio R_m of surfactant to salt making the micelles reach a maximum growth, i.e., $R_m \leq {}^1/_5$ for SDES/NaCl system, and $R_m \approx {}^1/_3$ for other three systems. The cations enhance micellar growth following the order of $Al^{3+} > Mg^{2+} > Ca^{2+} > Na^+$.

(v) The structure of SDES molecules makes micelles relatively easy to grow and form wormlike aggregates in the presence of inorganic salts. However, it is not clear which surfactants can form wormlike micelles under appropriate conditions. More experiments and theories should be made.

Acknowledgment. Financial support of this work by the National Natural Science Foundation of China (Grant 29973023) and State Laboratory of Oil and Gas Reservoir and Exploitation, Southwest Petroleum Institute of China, are gratefully acknowledged.

References and Notes

(1) Zana, R. *Surfactants Solutions: New Methods of Investigation*; Marcel Dekker Inc.: New York, 1987; p209.
(2) Hoffmann, H.; Rehage, H.; Rauscher, A. *Statics and Dynamics of Strongly Interacting Colloids and Supramolecular Aggregates in Solution*; Chen, H., et al., Eds.; Fliver Academic Publishers: Netherlands, 1992; p493.
(3) Rehage, H.; Hoffmann, H. *J. Phys. Chem.* **1988**, *92*, 4712.
(4) Khatory, A.; Kern, F.; Lequeux, F.; Appell, J.; Porte, G.; Morie, N.; Ott, A.; Urbach, W. *Langmuir* **1993**, *9*, 933.
(5) Berret, J. F. *Langmuir* **1997**, *13*, 2227.
(6) Ponton, A.; Schott, C.; Quemada, D. *Colloids Surf. A* **1998**, *145*, 37.
(7) Kumar, S.; Bansal, D.; Kabir-ud-Din *Langmuir* **1999**, *15*, 4960.
(8) Caudau, S. J.; Oda, R. *Colloids Surf. A* **2001**, *183*−*185*, 5.
(9) Vinson, P. K.; Bellare, J. R.; Davis, H. T.; Miller, W. G.; Scriven, L. E. *J Colloid Interface Sci.* **1991**, *142*, 74.
(10) Kern, F.; Zana, R.; Candau, S. J. *Langmuir* **1991**, *7*, 1344.
(11) Clausen, T. M.; Vinson, P. K.; Minter, J. R.; Davis, H. T.; Talmon, Y.; Miller, W. G. *J. Phys. Chem.* **1992**, *96*, 474.
(12) Khatory, A.; Lequeux, F.; Kern, F.; Candau, S. J. *Langmuir* **1993**, *9*, 1456.
(13) Shikata, T.; Imai, S.; Morishima, Y. *Langmuir* **1998**, *14*, 2020.
(14) Ali, A. A.; Makhloufi, R. *Colloid Polym. Sci.* **1999**, *277*, 270.
(15) Zheng, Y.; Lin, Z.; Zakin, J. L.; Talmon, Y. *J. Phys. Chem. B* **2000**, *104*, 5263.
(16) Fukada, K.; Suzuki, E.; Seimiya, T. *Langmuir* **1999**, *15*, 4217.
(17) Teipel, U.; Heymann, L.; Aksel, N. *Colloids Surf. A* **2001**, *193*, 35.

(18) Lin, Z. Q.; Zakin, J. L.; Talmon, Y.; Zheng, Y.; Davis, H. D.; Scriven, L. E. *J. Colloid Interface Sci.* **2001**, *239*, 543.
(19) Won, Y. Y.; Davis, H. T.; Bates, F. S. *Science* **1999**, *283*, 960.
(20) Shchipunov, Yu. A.; Hoffmann, H. *Langmuir* **1999**, *15*, 7108.
(21) Maeda, H.; Yamamoto, A.; Souda, M. *J. Phys. Chem. B* **2001**, *105*, 5411.
(22) Magid, L. J. *J. Phys. Chem. B* **1998**, *102*, 4064.
(23) Mishic, J. R.; Fisch, M. R. *J. Chem. Phys.* **1990**, *92*, 3222.
(24) Tokiwa, F. *J. Phys. Chem.* **1968**, *72*, 1214.
(25) Zhao, G. X.; Zhu, D. M. *China Surf. Det. Cos.* **1996**, *3*, 1.
(26) Jahn, W.; Strey, R. *J. Phys. Chem.* **1988**, *92*, 2294.
(27) Hoffmann, H.; Thunig, C.; Schmiedel, P.; Munkert, U. *Langmuir* **1994**, *10*, 3972.
(28) Gulik-Krzywichi, T.; Dedieu, J. C.; Roux, D.; Degert, C.; Laversanne, R. *Langmuir* **1996**, *12*, 4668.
(29) Hoffmann, H.; Ulbricht, W. *Tenside Surf. Det.* **1998**, *35*, 421.
(30) Gradzielski, M.; Muller, M.; Bergmeier, M.; Hoffmann, H.; Hoinkis, E. *J. Phys. Chem. B* **1999**, *103*, 1416.
(31) Mu, J. H.; Li, G. Z. *Colloid Polym. Sci.* **2001**, *279*, 872.
(32) Cross, M. M. *J. Colloid Sci.* **1965**, *20*, 417.
(33) Montalvo, G.; Valiente, M.; Rodenas, E. *Langmuir* **1996**, *12*, 5202.
(34) Nemeth, Zs.; Halasz, L.; Palinkas, J.; Bota, A.; Horanyi, T. *Colloids Surf. A* **1998**, *145*, 107.
(35) Alfaro, M. C.; Grerrero, A. F.; Munoz, J. *Langmuir* **2000**, *16*, 4711.
(36) Kern, F.; Lequeux, E.; Zana, R. *Langmuir* **1994**, *10*, 1714.
(37) Candau, S. J.; Hebrand, P.; Schmitt, V.; Lequeux, F. *Nuovo Cimento D* **1994**, *16*, 1401.
(38) Cates, M. E. *J. Phys. Chem.* **1990**, *94*, 371.
(39) Mitchell, D. J.; Ninham, B. W. *J. Chem. Soc. Faraday Trans. 2* **1981**, *77*, 601.
(40) Holtzclaw, H. F., Jr.; Robinson, W. R. *College Chemistry with Qualitative Analysis*, 8th ed.; D. C. Health and Company: Lexington, 1988; p 360.